Differential Search Coils Based Magnetometers: Conditioning, Magnetic Sensitivity, Spatial Resolution

Maria Timofeeva, Gilles Allègre, Didier Robbes, Stéphane Flament

Differential Search Coils Based Magnetometers: Conditioning, Magnetic Sensitivity, Spatial Resolution

[1] Timofeeva Maria, [1,2] Allegre Gilles, [1,2] Robbes Didier, [1,3] Flament Stéphane
[1] GREYC – UMR 6072, 6 Bd Mal Juin, 14050 CAEN Cedex, France
[2] Université de Caen, Bd Mal Juin, 14050 CAEN Cedex, France
[3] ENSICAEN, 6 Bd Mal Juin, 14050 CAEN Cedex, France
E-mail: sflament@ensicaen.fr

Abstract: A theoretical and experimental comparison of optimized search coils based magnetometers, operating either in the Flux mode or in the classical Lenz-Faraday mode, is presented. The improvements provided by the Flux mode in terms of bandwidth and measuring range of the sensor are detailed. Theory, SPICE model and measurements are in good agreement. The spatial resolution of the sensor is studied which is an important parameter for applications in non destructive evaluation. A general expression of the magnetic sensitivity of search coils sensors is derived. Solutions are proposed to design magnetometers with reduced weight and volume without degrading the magnetic sensitivity. An original differential search coil based magnetometer, made of coupled coils, operating in flux mode and connected to a differential transimpedance amplifier is proposed. It is shown that this structure is better in terms of volume occupancy than magnetometers using two separated coils without any degradation in magnetic sensitivity. Experimental results are in good agreement with calculations.

Keywords: Search coil sensor, Magnetometer, Magnetic, Sensitivity, Transimpedance amplifier, Spatial resolution.

---

1. Introduction

This research work takes place in the context of an industrial contract aiming at developing a robust small size (1 cm^3) large bandwidth magnetometer. We investigated benefits provided by using search coils operating in the flux mode, instead of the classical Lenz-Faraday mode. This paper consists in a theoretical and experimental comparative study of sensors specifications (bandwidth, sensitivity,

measuring range) depending on the operating mode. To meet the industrial constraints, we fixed a budget (i.e. we selected commercial ferrite cores and a low noise differential instrumentation amplifier). The obtained results are providing new solutions for applications requiring large bandwidth like pulsed eddy current non destructive evaluation [1], biomedical or geomagnetic measurements in the [1 Hz - 1 MHz] bandwidth, for which Lenz mode magnetometers are not well adapted. We present in section 2 the main characteristics of the sensors for the two operating mode. In Section III, we discuss how to optimize the signal conditioning so as to obtain low noise and large bandwidth magnetic field sensors. We show that using search coils in a Flux mode enables a large enhancement of both bandwidth and measuring range of the sensor without reduction of its sensitivity. Section 4 is devoted to the study of a coupled search coils sensor in Flux mode and the design of a small size differential coils based magnetometer. Sections 5 and 6 deal with the magnetic sensitivity of search coils sensors. We show that the magnetic sensitivity in Flux and Lenz mode are the same and detail which are the relevant parameter that fix the white noise level of the sensor as well as the noise corner frequency. Section 7, deals with the theoretical and experimental study of differential search coils magnetometers. A white noise level of $0.4\ pT/\sqrt{Hz}$ is obtained using $0.8\ cm^3$ differential coupled search coils. In section 8, the spatial resolution of search coils sensors is studied. We show that the resolution is not the same in Lenz and Flux mode.

2. Sensors Characteristics and Electrical Equivalent Model in Flux mode and Lenz Mode

In the Lenz mode, the search coil generates a voltage signal proportional to the flux time derivative not to the flux density Be and is connected to a voltage instrumentation amplifier with an infinite input impedance. In the flux mode, the short circuit current, proportional to the field density, is measured. In that case the coil has to be connected to an infinite input admittance transimpedance amplifier [2]. Thus, search coils sensor can be considered as voltage or current source depending of the mode they are being operated. Their Thevenin equivalent voltage generator E_{Th}, Thevenin impedance Z_{Th}, Norton equivalent current generator I_N and Norton equivalent admittance Y_N (Fig. 1) can be calculated as a function of both the flux density B_e to measure and the coil features: inductance L_b, noisy resistance R_b, parasitic capacity C_b and equivalent surface S_{eq}, which is defined as the ratio of the collected flux to the flux density Be and experimentally determined. One gets:

$$E_{Th} = \frac{e_{nRb} - j\omega B_e S_{eq}}{(1 - L_b C_b \omega^2) + j\omega R_b C_b}$$

$$Z_{Th} = \frac{R_b + j\omega L_b}{(1 - L_b C_b \omega^2) + j\omega R_b C_b}$$

$$I_N = \frac{e_{nRb} - j\omega B_e S_{eq}}{R_b + j\omega L_b} \quad \text{and} \quad Y_N = \frac{1}{Z_{th}}$$

where e_{nRb} stands for the Johnson voltage noise source of R_b.

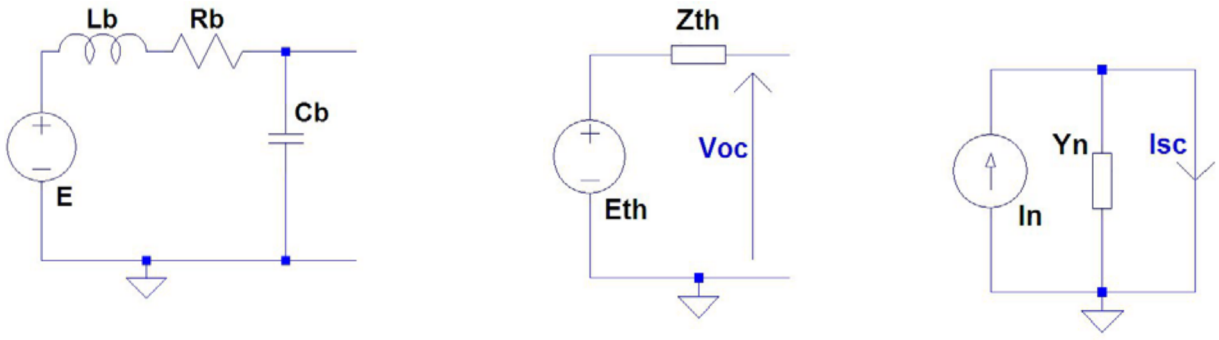

(a) (b) (c)

Fig. 1. Electrical equivalent circuit of a search coil (a), operating in Lenz mode (b), or Flux mode (c). In Lenz mode the magnetic flux is related to the open circuit voltage Voc whereas in Flux mode, the flux density is related to the short circuit current Isc.

The transfer functions $T_V = \frac{\partial E_{Th}}{\partial B_e}$ and $T_I = \frac{\partial I_N}{\partial B_e}$ and the intrinsic magnetic noise sensitivity, defined as the input noise flux density ($T/\sqrt{Hz}$) that produces a voltage (or current) equal to the contribution of the Johnson noise of the resistance R_b, are plotted as a function of the frequency in Fig. 2. One deduces from these figures that in the Lenz mode the bandwidth is intrinsically upper limited by the coil resonant frequency and that the measuring range is inversely proportional to the frequency, whereas in the flux mode the bandwidth is larger, since not affected by the coil resonant frequency, and the measuring range is constant above a low cut off frequency equal to $\frac{R_b}{2\pi L_b}$ [3]. The magnetic sensitivity in the Lenz mode decreases as the frequency and is thus better at high frequency than in the flux mode. In this latter case, the sensitivity is constant over the bandwidth sensor.

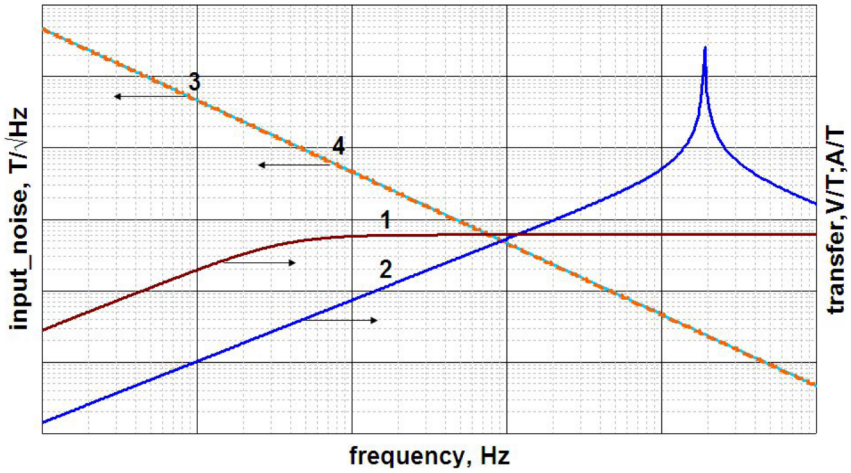

Fig. 2. Transfer function and intrinsic sensitivity of search coil magnetometer in Lenz mode (2 & 4) and Flux mode (1 & 3) as a function of the frequency.

As a brief conclusion, intrinsically, the flux mode sensor is well suited to applications requiring a large bandwidth and frequency independent measuring range whereas the Lenz mode magnetometer is rather adapted to applications in limited frequency range and provides in that case a better sensitivity than the Flux mode magnetometer.

Signal amplification is different depending on the operation mode of the search coil. The signal has to be amplified for the Lenz mode by a voltage amplifier, with as high as possible input impedance Z_i, and for the Flux mode Lenz mode by a transimpedance amplifier, with as large as possible input admittance Y_i. These amplifiers can be replaced by their equivalent noisy quadripolar model as shown on Fig. 3 and 4. Such models are very useful for calculating the effective sensitivity of the sensor taking into account the noise due to the amplifier stage and more generally to state the required characteristics of both search coils and amplifier for given sensor specifications in terms of bandwidth and sensitivity.

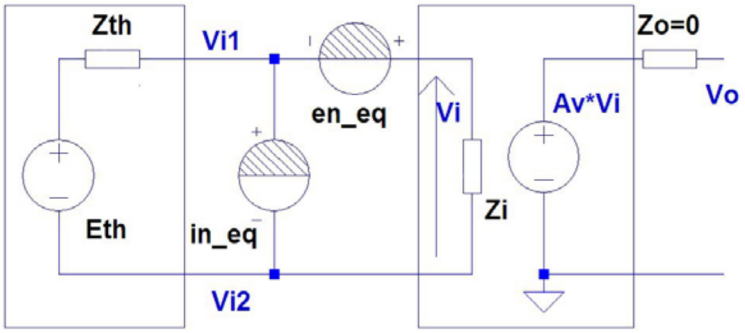

Fig. 3. Equivalent electrical model of the Lenz mode magnetometer. Av is the voltage Gain and Z_i the input impedance, which has to be as large as possible.

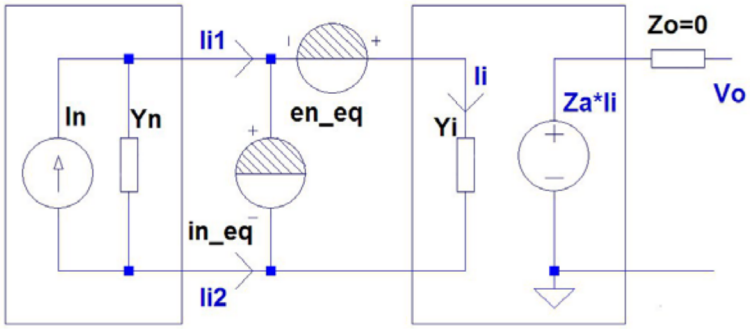

Fig. 4. Equivalent electrical model of the Flux mode magnetometer. Za is the amplifier transimpedance and Y_i is the input admittance, which has to be as large as possible

For signal conditioning, we selected an instrumentation amplifier structure (like the one included in the INA 163 integrated circuit) that we configurated so as to operate either as a voltage amplifier (for the Lenz mode) or as a transimpedance amplifier (for the Flux mode), as shown on Fig. 5 and 6.

3. Search Coils Sensors Conditioning Optimization

The classical Lenz mode magnetometer, which is rather a magnetic flux derivative meter, can be converted into a B field meter by using an integrator output stage [4]. We designed a solution with the integrator embedded inside the amplifier (Fig. 7). The transfer function T_{Lenz} of this Lenz mode B field meter is in that case given by:

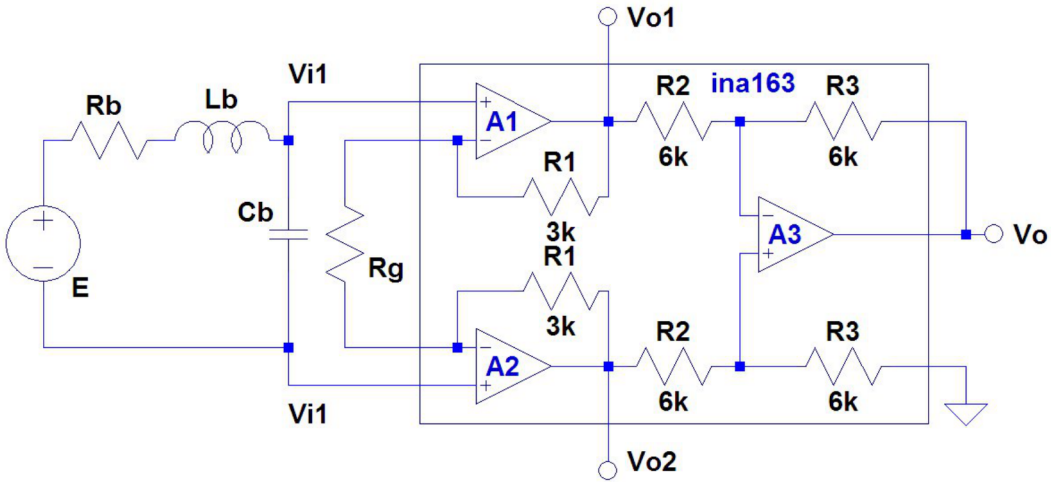

Fig. 5. Signal conditioning for Lenz mode magnetometer. Rg is the gain-set resistor.

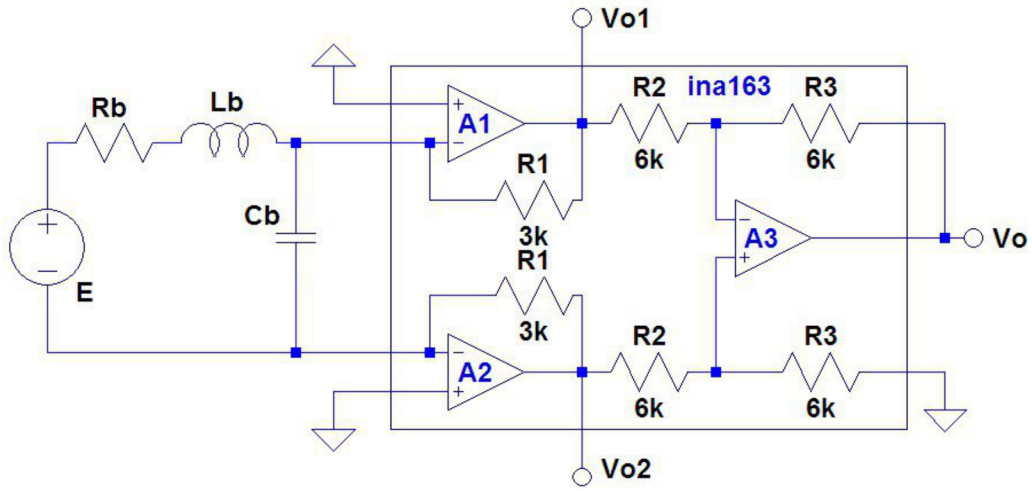

Fig. 6. Signal conditioning for Flux mode magnetometer

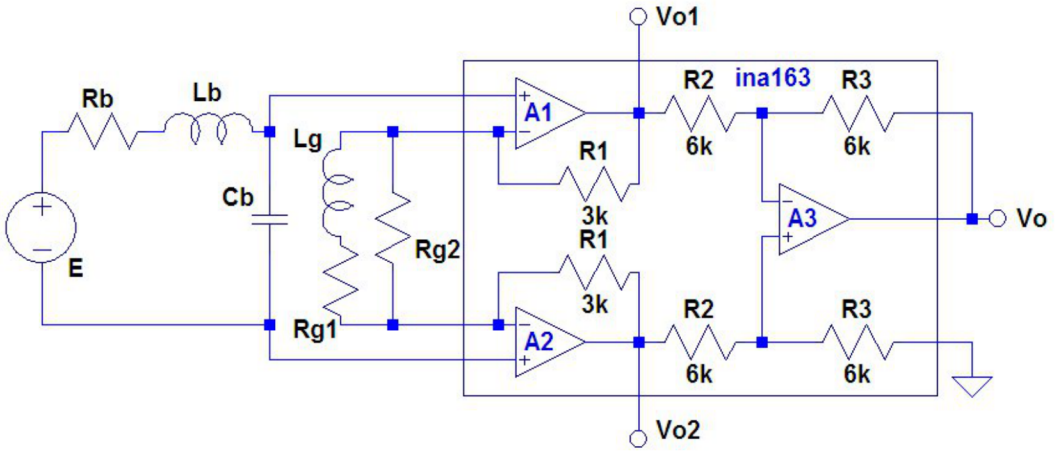

Fig. 7. Lenz mode B field meter with embedded integrator stage (Lg, Rg1 and Rg2), which replaces the gain-set resistor Rg in Fig. 5.

$$T_{Lenz} = \frac{\partial V_o}{\partial B_e} = \frac{j\omega S_{eq}}{1 - L_b C_b \omega^2 + j\omega R_b C_b}\left(1 + \frac{2R_1}{Z_g}\right)$$

where

$$Z_g = \frac{R_{g1}R_{g2}}{R_{g1} + R_{g2}} \cdot \frac{1 + j\omega\,\tau_{g1}}{1 + j\omega\,\tau_{g2}}$$

and

$$\tau_{g1} = \frac{L_g}{R_{g1}}\ , \qquad \tau_{g2} = \frac{L_g}{R_{g1} + R_{g2}}$$

The magnetometer low cut off frequency can be adjusted by proper choice of integrator parameters. Nevertheless, the magnetometer bandwidth is still limited by the search coils resonance and the measuring range is not enlarged by the integrator stage.

For the standard Flux mode magnetometer, the low cut off frequency is fixed by the search coil parameter. This low cut off frequency can be significantly reduced by including a compensation stage in the transimpedance amplifier as described in Fig. 8.

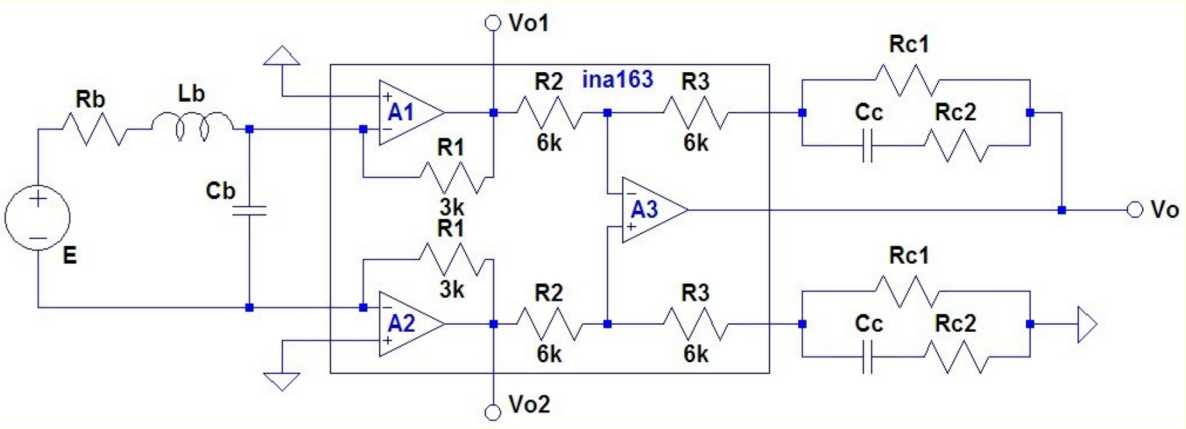

Fig. 8. Flux mode magnetometer with compensation stage (Rc1, Rc2 and Cc) for bandwidth enhancement at low frequency.

The function transfer T_{Flux} writes:

$$T_{Flux} = \frac{\partial V_o}{\partial B_e} = \frac{j\omega S_{eq}}{R_b(1 + j\omega\,\tau_b)} \cdot \frac{R_1}{R_2} \cdot \left(R_3 + \frac{R_{c1}(1 + j\omega\,\tau_{c2})}{(1 + j\omega\,\tau_{c1})}\right)$$

where

$$\tau_b = L_b/R_b\ ,\ \tau_{c1} = C_c\left(R_{c1} + R_{c2}\right),\ \tau_{c2} = C_c R_{c2}$$

Using the compensation stages described ahead, whatever is the mode of the magnetometer, one can obtained the same cut off low frequency and the same transfer value in the magnetometer bandwidth. The Lenz mode magnetometer bandwidth stays nevertheless limited by the search coil resonant frequency.

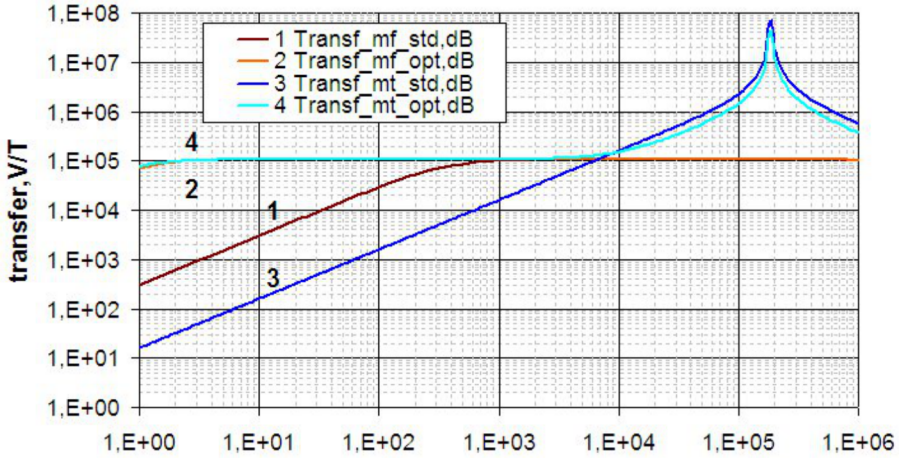

Fig. 9. Transfer function of standard (std 1 &3) magnetometer and optimized (opt 2 & 4) magnetometer.

4. Differential Coupled Search Coils Based Magnetometer

A significant reduction of common mode signals as well as parasitic signals sensed in connecting wires is usually achieved by the use of a differential structure. An original flux mode differential magnetometer is presented in Fig. 10. The Norton equivalent model and the transfer function of this magnetometer can be calculated as follows:

$$I_N = \frac{(e_{nRb1} + e_{nRb2}) - 2j\omega B_e S_{eq}}{2(R_b + j\omega(L_b + M))}, \qquad \frac{1}{Y_N} = \frac{2(R_b + j\omega(L_b + M))}{\left(1 - (L_b + M)C_b\omega^2\right) + j\omega R_b C_b}$$

$$T_{Diff} = \frac{\partial V_s}{\partial B_e} = \frac{2R_1R_3}{R_bR_2} \cdot \frac{pS_{eq}}{1 + \tau_{bd}p},$$

where

$$\tau_{bd} = \frac{L_b + M}{R_b} \text{ and } M = k\sqrt{L_{b1}L_{b2}}$$

The low cut off frequency can be significantly reduced by including the compensation stage described in Section III. The theoretical study was compared to experimental measurements and calculations using a SPICE simulator. All results are in good agreement as shown on Fig. 11.

The search coils coupling leads to correlation of the voltage noise sources of the two input amplifiers A_1 and A_2 of the instrumentation amplifier and thus to noise reduction of the sensor [5]. The coupling allows also a significant size reduction of the transducer since the coils can be wounded together on the same magnetic coil. In order to check the validity of the theoretical study, experimental measurements and calculations using a SPICE simulator were performed. All results fits very well as shown on Fig. 12.

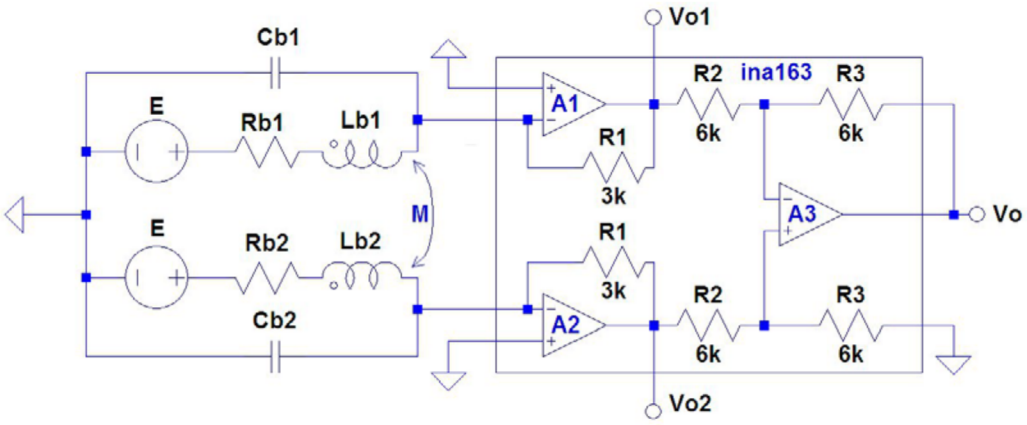

Fig. 10. Flux mode differential magnetometer structure.

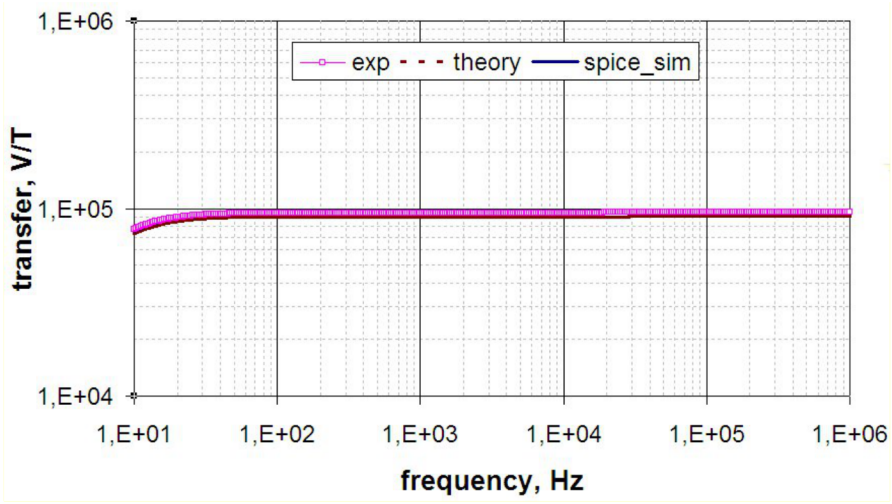

Fig. 11. Transfer function of the differential Flux mode magnetometer. Theoretical, experimental and SPICE simulation curves are in very good agreement. Search coils features are: $R_{b1} = R_{b2} = 45$ohms, $L_{b1} = L_{b2} = 4.7$ mH, $Cb_1 = Cb_2 = 60$ pF, $S_{eq} = 0.152$ m^2, Volume = 0.83 cm^3, intrinsic search coil transfer equal to 28A/T and search coil low cut off frequency equal to 1,5kHz. The compensation stage of the magnetometer (see Section III) was designed so as to obtain an 8 Hz low cut off frequency.

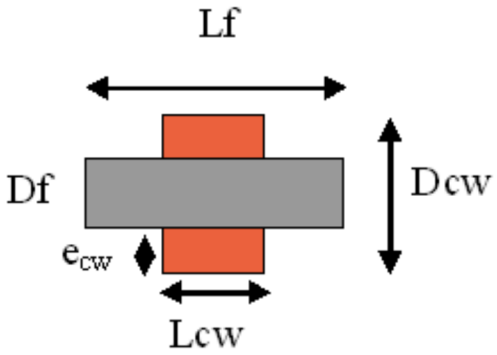

Fig. 12. Section view of the search coil. Subscripts 'cw' and 'f' stand respectively for Coil Wire and Ferrite core.

5. Intrinsic Search Coils Magnetic Sensitivity

The sensitivity of the sensor is limited by the Johnson noise of the coil resistance R_b. In a frequency band Δf, the variance of the noise voltage e_{nRb}^2 due to R_b is equal to:

$$e_{nRb}^2 = 4k_B T.R_b.\Delta f$$

From Faraday's law, signal power can be written as :

$$e_\Phi^2 = (S_{eq}\,\omega B_e)^2$$

Thus, for a signal to noise ratio equal to 1, one can define [6] the intrinsic magnetic induction resolution per unit bandwidth $B_n^{intrinsic}$ as :

$$B_n^{intrinsic} = \frac{\sqrt{4\,k_B T}}{\omega}\frac{\sqrt{R_b}}{S_{eq}} \qquad (T/\sqrt{Hz}) \tag{1}$$

One has now to express the resistivity and the equivalent area of the search coil depending on the geometry. Let's consider a search coils with geometrical parameters depicted in Fig. 12. We define forms factors m_f and m_{cw} for respectively the ferrite core and the coil wiring as :

$$m_f = L_f / D_f \quad \text{and} \quad m_{cw} = L_f / D_{cw}\ .$$

The resistance R_b expresses as :

$$R_b = N \cdot \frac{\rho.2\pi.r_{mean}}{S_w}$$

where S_w is the wire section, r_{mean} is the mean radius of the coils wiring i.e.

$$r_{mean} = \frac{D_{cw} + D_f}{2} = \frac{m_f + m_{cw}}{m_{cw}} \cdot \frac{D_f}{2}$$

and

$$N = k_{fill}\frac{L_{cw}.e_{cw}}{S_w},$$

(where k_{fill} is the packing factor which will be taken equal to 1).

The equivalent surface S_{eq}, can be expressed as:

$$S_{eq} = N.\mu_{app}.S_f,$$

where

$$S_f = \frac{\pi D_f^2}{4}$$

and where μ_{app} is the apparent permeability which is different from the relative permeability μ_r of the core due to the demagnetizing field. For an isotropic magnetic material ferrite,

$$\frac{1}{\mu_{app}} = \frac{1}{\mu_r} + N_d$$

where N_d is the demagnetizing factor. Assuming that the magnetic induction is constant inside the core and that the tube core can be considered as an ellipsoid, a general formula for N_d exists. [7]. Most existing papers deal with elongated search coils with $m_f > 10$. In this case, the apparent permeability, we note $\mu_{app,long}$ can be expressed by [4]:

$$\mu_{app,long} = \frac{L_f^2}{D_f^2} \cdot \frac{1}{\ln(2m_f) - 1} \cdot m_f$$

For compact coils ferrite with $0.5 < m_f < 4.5$, we propose a simple expression for N_D. N_D can be approximated with less than 15 % error by:

$$N_d \approx \frac{1}{\pi m_f} = \frac{1}{\pi} \frac{D_f}{L_f} \quad .$$

In this case, the apparent permeability, we note $\mu_{app,short}$, reduces to:

$$\mu_{app,short} \approx \pi m_f$$

As a result, the intrinsic magnetic induction resolution $B_n^{intrinsic}$ expression for short and long coils expression are:

$$B_{n,short}^{intrinsic} = \frac{8\sqrt{k_B T \rho}}{\pi \omega} \cdot \frac{m_f + m_{cw}}{m_{cw}} \cdot \frac{1}{L_f \sqrt{V_{copper}}} \tag{2}$$

$$B_{n,long}^{intrinsic} = \frac{8\sqrt{k_B T \rho}}{\pi \omega} \cdot \frac{m_f + m_{cw}}{m_{cw} \cdot} \cdot \frac{\pi^2 \left[\ln(2m_f) - 1\right]}{m_f} \cdot \frac{1}{L_f \sqrt{V_{copper}}} , \tag{3}$$

where V_{copper} is the coil wiring volume: $V_{copper} = 2\pi . r_{mean} \cdot L_{cw} \cdot e_{cw}$

The main conclusion is that, whatever the coil geometry, the sensitivity is mainly governed by the length of the core and the copper volume.

6. Effective Magnetic Sensitivity of the Sensor

6.1. Scale Factors

For any search coils magnetometer, an open voltage is induced in the coil and one can then define a transfer function or Voltage Scale Factor SF_V as:

$$SF_V = \frac{E_{th}}{B_{ext}} = S_{eq} \cdot \omega = N.\mu_{app}.S_f.\omega \tag{4}$$

$$SF_V \approx \frac{\pi^2}{4} \cdot N\, L_f\, D_f\, \omega \quad (\text{for short core}) \tag{5}$$

In Flux mode, the induced short circuit current I_N is measured using a transimpedance amplifier with high input admittance larger than the one of the coil capacitance. Their transfer function or current (Intensity) Scale Factor SF_I is then defined as:

$$SF_I = \frac{I_N}{B_{ext}} = \frac{e_\Phi}{R_b + jL_b\omega} \cdot \frac{1}{B_{ext}} = \frac{SF_v}{R_b + jL_b\omega} \tag{6}$$

where L_b is the search coil inductance. This latter can be expressed as:

$$L_b = \mu_o.\mu_{self}.N^2 \cdot \frac{S_f}{L_f} \tag{7}$$

where μ_{self} is an apparent permeability, corresponding to the field enhancement due self induction, equal to the ratio of the inductances values for a solenoid with and without ferrite core. On the assumption that the field produced by the coil wiring is uniform and that magnetization inside the ferrite is uniform, μ_{self} and μ_{app} are usually considered to be equal [4] even if finite element calculations are required for a more accurate evaluation of their ratio. As a result, for a frequency above $f_c = \frac{R}{2\pi L_b}$, SF_I is frequency independent and simplifies to:

$$SF_I = \frac{\Phi}{L_b \cdot B_{ext}} = \frac{S_{eq}}{L_b} = \frac{N\,\mu_{app}\,S_f}{N^2\,\mu_o\,\mu_{self}\,S_f/L_f} \approx \frac{L_f}{N\mu_0} \tag{8}$$

6.2. Effective Magnetic Sensitivity

The effective magnetic sensitivity of the sensor depends on the noise characteristics of the preamplifier [8]. As explained before, in the Lenz mode a high input impedance voltage amplifier is used, in flux mode a high admittance current amplifier or transimpedance amplifier is used (Fig. 13).

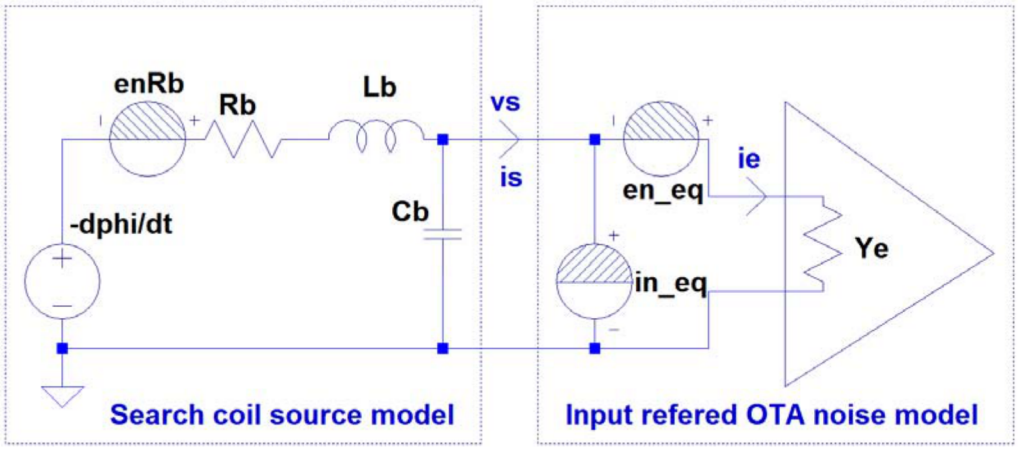

Fig. 13. Search coil magnetometer operating in Flux mode. $e_{n\text{-}eq}$ and i_{n_eq} are equivalent input voltage and current noise of the pre-amplifier whose input admittance is Ye.

Below the coil resonance frequency for the Lenz mode magnetometer, the equivalent input noise voltage e_{n_eq} is equivalent to a magnetic induction noise e_{n_eq}/SF_V and the equivalent input noise current i_{n_eq} is equivalent to a magnetic induction noise i_{n_eq}/SF_I . As a result the effective magnetic induction sensitivity is:

$$B_n^2 = B_n^{2\text{int rinsic}} + \frac{e_{n\_eq}^2}{SF_v^2} + \frac{i_{n\_eq}^2}{SF_I^2} = B_n^{2\text{int rinsic}} + \frac{1}{S_{eq}^2}\cdot\frac{e_{n\_eq}^2\cdot}{\omega^2} + \cdot\frac{L_p^2}{S_{eq}^2}\cdot i_{n\_eq}^2 \tag{9}$$

$$B_n^2 \approx B_n^{2\text{int rinsic}} + \frac{1}{S_{eq}^2}\cdot\frac{e_{n\_eq}^2\cdot}{\omega^2} + \mu_o^2\cdot\frac{N^2}{L_f^2}\cdot i_{n\_eq}^2 \tag{10}$$

6.3. Discussion

We deduce from equation 2 that minimization of the intrinsic magnetic induction sensitivity requires as large as possible copper volume and long ferrite core (high value of L_f). The number of turns N is not a relevant parameter. N becomes a relevant parameter when the noise of the amplifier is taken into account. In that case, equation (10) shows that, for any coil, the white noise level is fixed by the number of wires, the length of the core and the equivalent input current noise and is the same for air coils sensors and ferrite core sensors, since it does not depend on the apparent permeability. The value of N is indeed adjusted so as to meet the required specifications of the sensor in terms of magnetic noise sensitivity and bandwidth of the white noise region. The reason is that the noise corner frequency f_{corner} for which the noise due to e_{n_eq} becomes smaller than the noise due to i_{n_eq} is equal to:

- for short coils:

$$f_{c\_noise\_short} = \frac{e_{n\_eq}/i_{n\_eq}}{\mu_o\,\pi\,N^2}\cdot\frac{1}{D_f}\cdot\frac{4}{\pi}f \tag{11}$$

- for long coils:

$$f_{c\_noise\_long} = \frac{e_{n\_eq}/i_{n\_eq}}{\mu_o \pi N^2} \cdot \frac{1}{L_f} \cdot \frac{4}{\ln(2\, m_f) - 1} \qquad (12)$$

and depends on the apparent permeability.

7. Differential Search Coils Based Magnetometer

Differential sensors are the most appropriate one for getting rid with parasitic signals. In the case of magnetic sensors, a typical parasitic signal is the flux collected by the connection wires to the amplifier. It is possible to remove this flux by the use of two identical search coils sensors thus providing a differential sensor but with a less spatial resolution. If one wants to optimize size as well as spatial resolution, one can put the two sensors together to obtain a single differential sensor. By using two identical coils wounded on the same ferrite core and operating in flux mode (the coils are then highly coupled), one gets a magnetometer based on a differential sensor. The short circuit current (proportional to B_{ext}) of both search coils is added using the differential current amplifier whereas the flux picked up in the connection wiring can easily be removed by an appropriate wounding of theses wires. If L_{coil} is the inductance of one of the two coupled coils and S_{coil} its equivalent surface, it can be shown that the signal produced by two identical coupled coils is the same as the one produced by an equivalent coil with inductance $L_{cc} = L_{coil} + M \approx 2\, L_{coil}$ (where M is the mutual inductance between the coil which very close to L_{coil}) and equivalent surface value $S_{eq\_cc} = S_{coil}$. Let's compare the sensitivity of such two coupled search coils with the sensitivity of two identical but separated coils of half length, the same copper and ferrite volumes are then used for both sensors. The equivalent surface of each single coil wounded onto the ferrite of half length is $S_{eq\_cc} = S_{coil}/2$ and their inductance is $L_{cc}/2$. Thus from equation (10), we deduce that the white noise should be the same for both sensors whereas, from equation (11), the noise corner noise frequency should differ by a factor of 2. This was confirmed experimentally as shown on Fig. 14. We measured the magnetic induction sensitivity of coupled coils consisting of two coils with N = 400 turns, wounded on a ferrite 10 mm long, 4 mm in diameter with μ_r=900 and compared it with a magnetometer made of two separated coils wounded on a ferrite 5mm long, 4mm in diameter with $\mu_r = 900$. The measured white noise level is $0.4\, pT/\sqrt{Hz}$ in both cases. Using a calculated value of $2.3\, pA/\sqrt{Hz}$ for i_{n_eq}, (deduced from typical noise sources values available in data sheets of the integrated circuit used for designing the transimpedance amplifier) and measured values $S_{coil} = 0{,}035\ m^2$ and $L_{coil} = 4.5\, mH$, one gets from equation (9) a value of $0.3\, pT/\sqrt{Hz}$ and from equation (10) a value of $0.25\, pT/\sqrt{Hz}$. The small differences can be explained first from the fact that i_{n_eq} was not measured experimentally and second, for equation (10), from the fact that we considered that the core was equivalent to an ellipsoid.

8. Search Coils Sensors Spatial Resolution

Due to the presence of a ferrite core, the flux density distribution closed to the coils is different from the one when the coil is not present. It is thus interesting to estimate on which scale this modification takes place. The changes are not the same for the Lenz and the Flux mode. The reason why is that in the Flux mode eddy currents are induced in the wirings which generate a flux opposite to the one applied to the wirings. In order to evaluate the spatial resolution of search coils sensors, we calculated the flux density distribution around them when a uniform flux density B_{ext} is applied along the core length. We decided to define the spatial resolution as the extent of the region for which the flux density is either 5 % above or below the applied field. Fig. 15 show the results obtained for a few search coils

with a fixed length core L_f but with different core diameters D_f. In Lenz mode, the conclusion is that the spatial resolution along the direction of the applied field is not strongly affected by the ratio of the length over the diameter and ranges between 0.5 L_f and 1,5 L_f. We also compared the flux density distribution obtained for solid and hollow cores (Fig. 16). It turns out that the spatial resolution and the equivalent surface are the same in both case, which a very interesting result in term of weight reduction and optimal use of the volume. As shown on Fig. 17, in the Flux mode, the spatial resolution along the direction of the applied field does not depend of the core shape factor and is about 0.5 L_f.

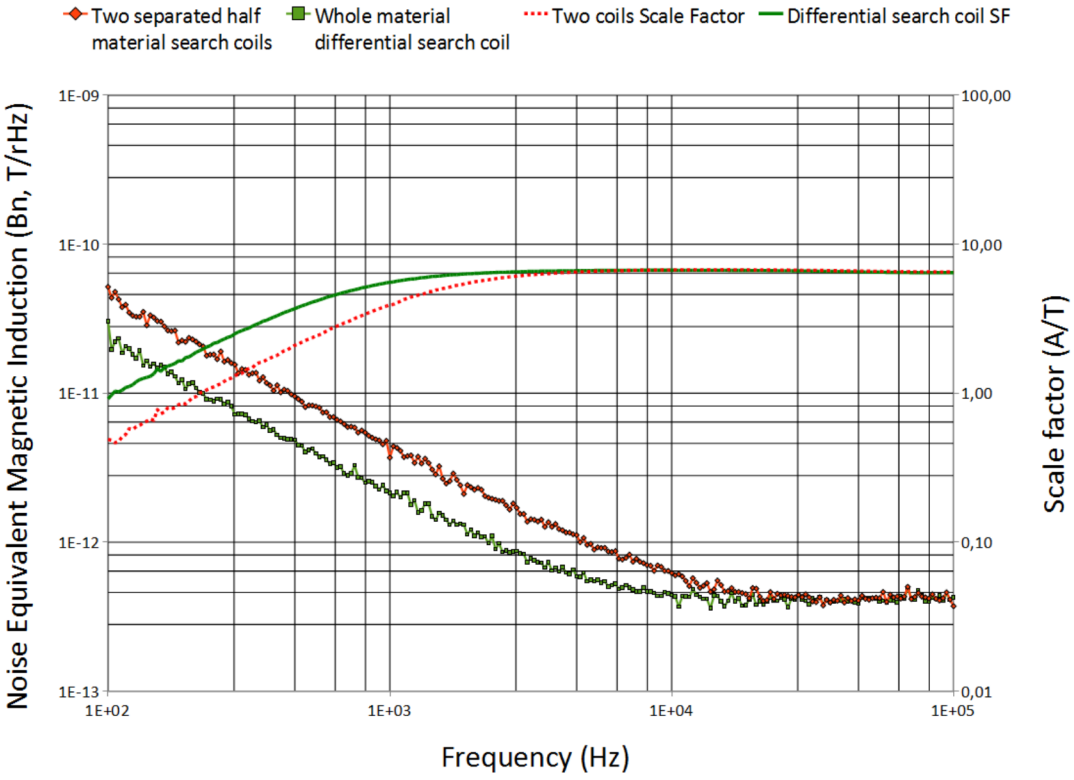

Fig. 14. Scale Factor and Noise equivalent Magnetic induction of sensitivity density per unit bandwidth of search coil magnetometers operating in Flux mode, made of two coils either coupled (green curves) or uncoupled (red curves). The same volume of ferrite and wiring is used for both magnetometers as well as the same transimpedance amplifier.

5. Conclusions

A detailed comparison of transfer function and noise sensitivity of search coils magnetometer operating either in Lenz mode of Flux mode was presented. We explained how to optimize both magnetometers and showed that the Flux mode provides a transfer function, which can be set constant over a bandwidth ranging from 1 Hz to 1 MHz, larger than what can be achieved in Lenz mode. The Flux mode also provides a constant measuring range over the full bandwidth, which is not the case for Lenz mode magnetometer. Such features are very interesting for applications requiring a large bandwidth and a good sensitivity over the whole bandwidth. An original differential coils based flux mode magnetometer, which is more compact than classical Lenz mode search coil differential magnetometer, was proposed and studied in details, namely in terms of transfer function and noise. Theoretical analysis, SPICE simulations and experimental measurements are in good agreement.

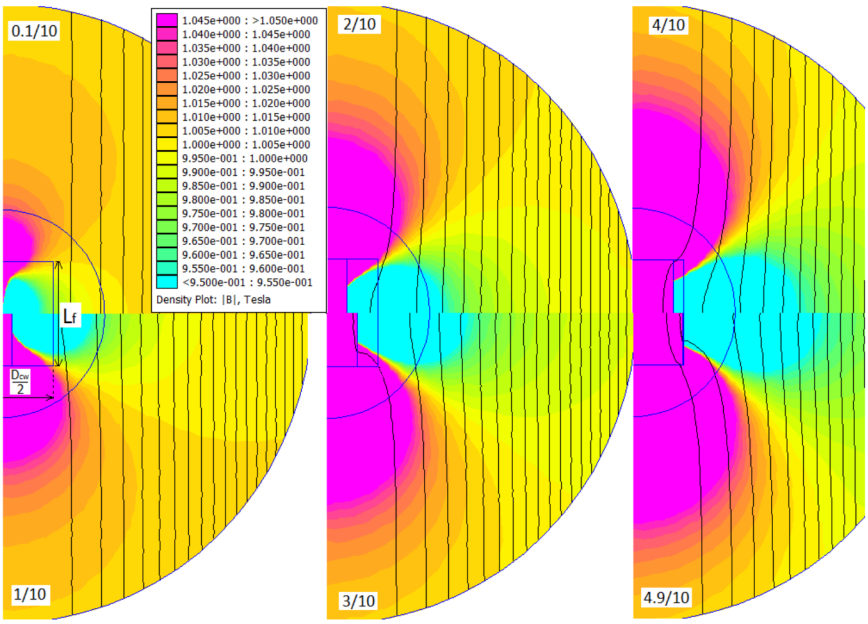

Fig. 15. Comparison of magnetic induction distribution (in μT) around rod type ferrite cores for a uniform flux density applied along the length of the core and equal to 1μT. FEMM software was used for calculations. The ferrite length L_f is 10 mm and the diameter D_f range from 0.2 mm to 8 mm. The ratio in the insert corresponds to $D_f/2L_f$. Thanks to the symmetry of the field distribution, each image is divided in two parts, an upper one and the lower each corresponding to a different $D_f/2L_f$. ratio. Pink region correspond to region where the flux density is more than 5 % above the applied flux density. Turquoise blue region correspond to region where the flux density is more than 5 % below the applied flux density.

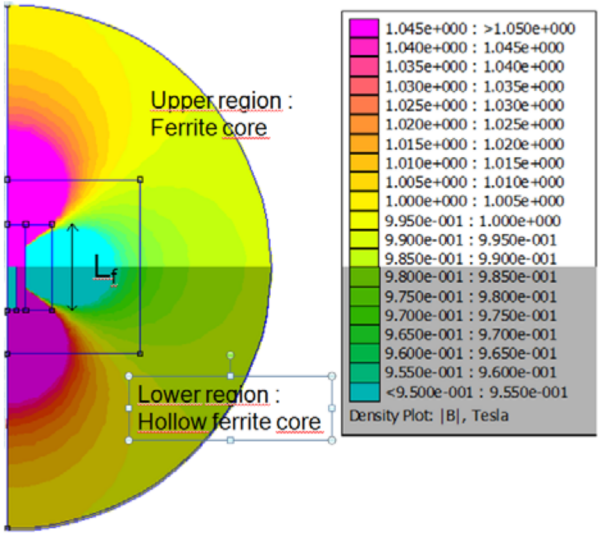

Fig. 16. Comparison of magnetic induction distribution (in μT) around ferrite cores for a uniform applied flux density equal to 1μT. FEMM software was used for calculations. The ferrite length L_f is 10 mm and the diameter D_f is 4 mm. The coils wiring length is L_f and its outside radius is 5 mm. The half upper part shows the flux distribution produced by a solid ferrite core. In the half lower part of the caption, the flux distribution produced by a solid ferrite core was replaced the one produced by a hollow ferrite core with a hole diameter of 2 mm. Pink region correspond to region where the flux density is more than 5 % above the applied flux density. Turquoise blue region correspond to region where the flux density is more than 5 % below the applied flux density. Outside the ferrites, the field distributions are very similar for both cases. Though different values of μ_{app} for the two cases, the calculated flux through the wiring (N=400) are the same (equal to 160 pWb) and thus the equivalent surface Seq are the same in both case (0.07 m^2).

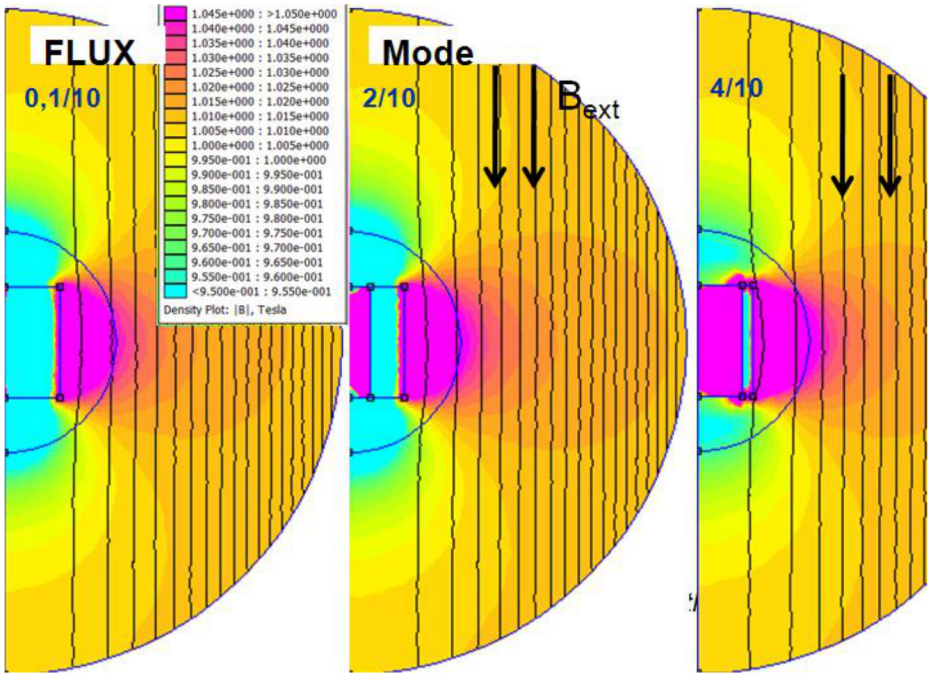

Fig. 17. Comparison of magnetic induction distribution (in μT) around rod type ferrite cores for a uniform flux density applied along the length of the core and equal to 1μT. FEMM software was used for calculations. The ferrite length L_f is 10 mm and the diameter D_f range from 0.2 mm to 8 mm. The ratio in the insert corresponds to $D_f/2L_f$. The coils wiring length is L_f and its thickness ranges from 4.9 down to is 1 mm. Pink region correspond to region where the flux density is more than 5 % above the applied flux density. Turquoise blue region correspond to region where the flux density is more than 5 % below the applied flux density.

Taking into account the Johnson noise of the coils as well as the electrical noise of the conditioners, we calculated the magnetic sensitivity of search coils magnetometers and showed that the white noise level only depends on the number of turns and of the wirings, the length of the coils and the equivalent input noise current of the conditioner. The equivalent surface of search coils sensor as a function of the core diameter was studied as well as the spatial resolution of the sensor for Lenz and Flux mode. The main results are first that hollow ferrite cores provides equivalent surface and spatial resolution similar to the ones of solid cores and second that the flux distribution around search coils is not the same for Lenz and Flux modes. The spatial resolution slightly depends on the core diameter and is about the length of the core.

References

[1]. C. Dolabdjian, L. Perez, V. O. De Haan and P. A. De Jong, Performance of Magnetic Pulsed-Eddy-Current System Using High Dynamic and High Linearity Improved Giant Magneto Resistance Magnetometer, *IEEE Sensors Journal*, Vol. 6, No. 6, 2006, pp. 1511-1517.

[2]. M. Timofeeva, G. Allègre, S. Flament and D. Robbes, Des lois de l'induction aux théorèmes de thévenin et Norton, *CETSIS,* 2010.

[3]. R. J. Prance, T. D. Clarke and H. Prance, Compact broadband gradiometric induction magnetometer system, Sensors and Actuators, 76, 1999, pp. 117-121.

[4]. S. Tumanski, Induction coil sensors-a review, *Measurement Science and Technology,* 18, 2007, pp. R31-R46.

[5]. M. Timofeeva, G. Allegre, D. Robbes, J. Gasnier and S. Flament, Input noise model of differential amplification structure and application to magnetic sensitivity evaluation of search coils magnetometers, submitted to *IEEE Sensors,* 2011.

[6]. Coillot, J. Moutoussamy, R. Lebourgeois, S. Ruocco and G. Chanteur, Principle and Performance of a Dual-Band Search Coil Magnetometer: A New Instrument to Investigate Fluctuating Magnetic Fields in Space, *IEEE Sensors Journal,* Vol. 10, No. 2, 2010, pp. 255-260.
[7]. J. A. Osborn, Demagnetizing Factors of the General Ellipsoid, *Phys. Rev.,* Vol. 67, No. 11&12, 1945, pp. 351-357.
[8]. S. A. Macintyre, A Portable Low Noise Low Frequency Three-Axis Search Coil Magnetometer, *IEEE Trans. Mag.,* Vol. 16, No. 5, 1980, pp. 761-763.